J. Plasma Fusion Res. SERIES, Vol. 5 (2002) 584–587

ECH Power Modulation Experiments in LHD

KUBO Shin, IDEI Hiroshi, SHIMOZUMA Takashi, YOSHIMURA Yasuo, NOTAKE Takashi[1],
OHKUBO Kunizo, INAGAKI Shigeru, NAGAYAMA Yoshio, NARIHARA Kazumichi
and LHD Experimental Group
National Institute for Fusion Science, Toki 509-5292, Japan
[1]Dept. of Energy Engineering and Science, Nagoya University, Nagoya 464-8603, Japan

(Received: 21 December 2001 / Accepted: 5 July 2002)

Abstract

Power deposition profile is one of the essential keys in understanding the transport mechanism in the plasma confinement devices. Using the power modulation techniques, the power deposition profile and its change in shape and position by the focal position is clearly observed experimentally in Large Helical Device (LHD). These power deposition profiles show fairly in good agreement with the results from ray tracing calculation. Such experimentally observed power deposition profiles are used as the inputs of newly developed one dimensional time dependent electron transport code to deduce the dynamic electron heat diffusivity that reproduces the experimental data.

Keywords:
modulation, transient analysis, transport, ECH, LHD

1. Introduction

The specific features of the electron cyclotron heating (ECH) are the capabilities that electrons can be heated selectively and locally in both real and velocity space. These features are fully utilized in LHD.

The fundamental and second harmonic ECH have been used as a main plasma production and electron heating method in the LHD. Recently, four gyrotrons at the frequency range of 84 GHz and three at 168 GHz are used to inject total power of more than 1 MW in LHD. The high central electron temperature, T_{e0}, of more than 10 keV is achieved by concentrating almost all the power in the central region near the axis within ($\rho \sim 0.2$). The averaged electron density region was up to $\sim 0.6 \times 10^{19}\,\mathrm{m}^{-3}$ when T_{e0} reached 10 keV. The sharp temperature gradient is normally observed in those high temperature plasma. These are closely related to the sharp power deposition profile and the change in the local confinement in the plasma.

The conditions of the magnetic configuration, the field strength and the focal points are the essential factors to get a required power deposition profile. The ECH system in LHD had been designed so that the power deposition profile would be as narrow as possible. The quasi-optical antenna system is used to focus the injected beam on the mid-plane with the width of 15 mm as a Gaussian beam waist size.

To understand the heat transport properties in such high temperature, low density region, it is of much importance to know the power deposition profile, in particular, the structure of the power deposition profiles in the central region. The square wave power modulation experiment at the frequency of 50 Hz for both the fundamental and the second harmonic heating are described in Sec. **2**. Here, the deduced power deposition profile using the boxcar averaging method is compared with the ray tracing result.

A simple one dimensional time dependent electron heat transport analysis code under such experimental

Corresponding author's e-mail: kubo@LHD.nifs.ac.jp

condition is developed to deduce the power deposition profile, electron heat diffusivity including its dependence on the temperature and the gradient of electron temperature. The thermal diffusivity and its dependence on the local temperature and local temperature gradient are discussed by comparing the observed ECE response and the simulated one qualitatively in Sec. **3**.

2. Modulation Experiments

The modulation experiments described here are performed at the averaged electron density of 1.0×10^{19} m^{-3} with flat profile. The electron temperature of parabolic profile and $T_{e0} \approx 2.5$ keV is sustained by NBI. The magnetic field is set at 2.951 Tesla and magnetic axis at 3.50 m. The fundamental and second harmonic resonance layers just cross the magnetic axis under this condition. Both heating powers are injected from the upper port antenna in the vertically elongated poloidal cross section. The 32 channel electron cyclotron emission (ECE) radiometer system is used to diagnose the local temperature response to the modulated ECH power. The viewing chord of the ECE radiometer is on the mid-plane of the horizontally elongated cross section. The direction of the beam injection is labeled by the radial focal position, R_{foc}, where the center of the injected beam crosses the mid-plane. Under the same magnetic field, the radial position and shape of the cross section between resonance layer and injected beam can be varied by changing the R_{foc}. Both injected powers have elliptical Gaussian beam shape. The waist sizes of each beam are 15 mm and 50 mm in radial and toroidal direction, respectively. The modulated power of both the fundamental and the second harmonic heating is applied on this target plasma. The fundamental heating power of 255 kW at the 82.7 GHz is applied from t = 1.02 to 1.42 s with the 100 %, 50 Hz square wave power modulation at the latter 300 ms of the pulse. The second harmonic heating power of about 400 kW at 168 GHz is applied from t = 1.52 to 1.92 s with the identical modulation as the fundamental heating. In Fig. 1 are shown the time response of ECE radiometer channels. Here, the cases of R_{foc} = 3.55 m and 3.4 m are shown in a) and b), respectively.

In the case of R_{foc} = 3.55 m of the fundamental heating, the central part of the electron temperature shows the fast response to the modulation, while it shows almost no response in the case of R_{foc} = 3.40 m. In order to see the spatial response in time, the fundamental heating part is re-plotted as the equi-temperature contours in the normalized radius, ρ, and time plane in Fig. 2 for these two cases. It is clearly seen that the region where the electron temperature show the fast response is center localized within ρ = 0.2. In case of R_{foc} = 3.40 m, the fast response is seen in the region from ρ = 0.2 to 0.6.

The boxcar technique is used for ±3 ms data points at every turn on and off timings [1,2] to deduce the first order power deposition profile. The differences of the inclination of each ECE channel are plotted as a function of normalized radius in Fig. 3 a) for the cases of R_{foc} = 3.55, 3.53, 3.45 and 3.40 m. The label "up" and "down" correspond to those estimated at turn-on and off timings, respectively. Here, the differences of the inclination (eV/s) are multiplied by the local density (m^{-3}), factors (3/2 and e), and normalized radius to represent the total power deposited at each flux surface. The power deposition profile is compared with the result from ray tracing calculations. The ray tracing code used here calculates the power deposition profile summing up the deposition fraction of multi-ray using the quasi

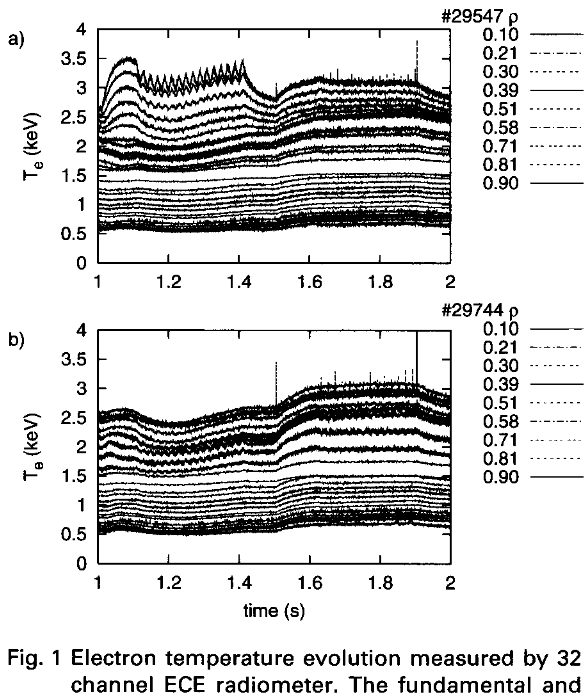

Fig. 1 Electron temperature evolution measured by 32 channel ECE radiometer. The fundamental and second harmonic ECH are applied from t = 1.02 to 1.42 and 1.52 to 1.92, respectively. The 50 Hz square wave modulation is applied at the latter 300 ms of each pulse. The focal point is set at a) 3.55 m and b) 3.40 m. The other injection conditions and the target plasma parameters are kept constant.

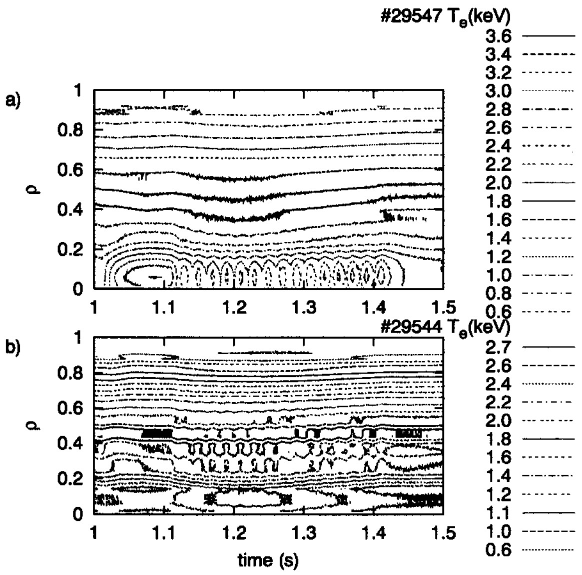

Fig. 2 Equi-electron temperature contour measured by 32 channel ECE radiometer. The focal point is set at a) 3.55 and b) 3.40 m. The other injection conditions are kept constant.

perpendicular, weakly relativistic absorption formula [3]. Each ray is calculated using the cold plasma dispersion. The ray start points are distributed on the real equi-phase plane so that each ray represents the same area within two times of the waist size there. The ray starting direction is taken to be perpendicular to the equi-phase plane. The Gaussian weighting function is convoluted to sum up the deposition profile. The Gaussian beam parameters and beam position are taken as the same as the designed values of the antenna, which are confirmed by the low power testing [2]. Both the deduced and the calculated power deposition profiles and those peak positions change correspondingly as the focal point is varied, although the peak positions for both are shifted about 0.1 in averaged radius. The discrepancies between calculated and deduced profiles in 168 GHz case may indicate the limitation of the ray tracing calculation using geometrical optics. The calculated power deposition profile is more sensitive to the antenna and resonance configuration for 168 GHz injection.

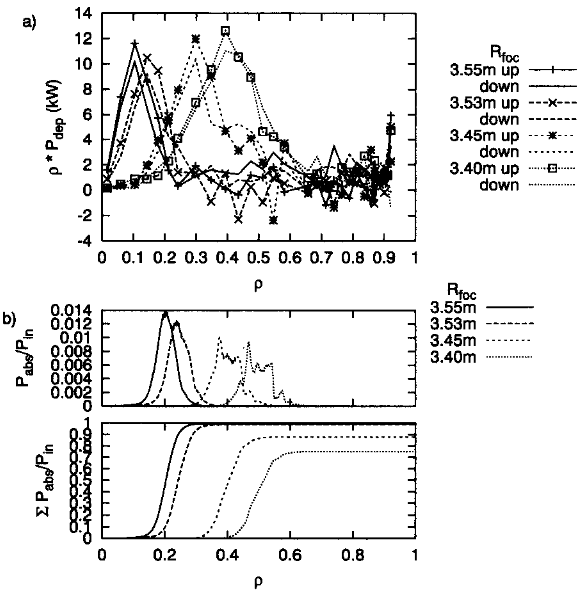

Fig. 3 a): Power deposition profile for 82.7 GHz estimated from boxcar method for R_{foc} = 3.40, 3.45, 3.53 and 3.55 m. The sample data are restricted within ±3 ms at each turn on and off timings in order to reduce the diffusion effect.
b): Power deposition profile (upper traces) and total absorption fraction within given flux surface (lower traces) estimated from ray tracing calculation for 82.7 GHz.

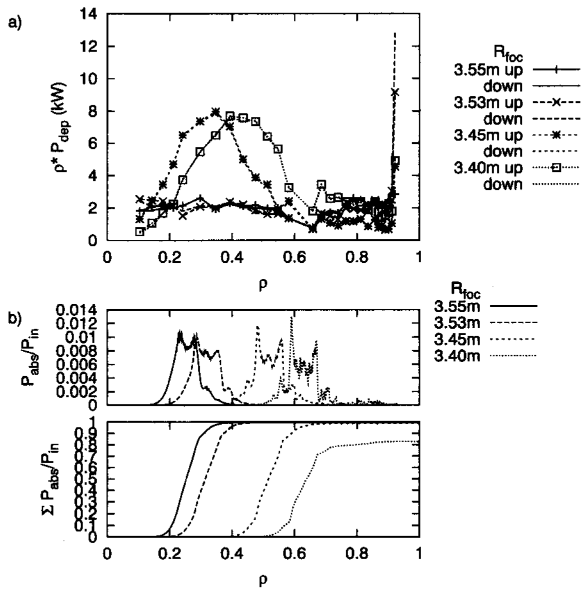

Fig. 4 a): Power deposition profile for 168GHz estimated from boxcar method for R_{foc} = 3.40, 3.45, 3.53 and 3.55 m. The sample data are taken as the same as the case for Fig. 3 a).
b): Power deposition profile (upper traces) and total absorption fraction within given flux surface (lower traces) estimated from the ray tracing calculation for the 168 GHz.

In Fig. 4 are shown the deduced and calculated power deposition profiles for the similar focal point settings in the case of 168 GHz modulation. The central ECE channels are affected by the stray of the gyrotron power and are not available. This shift might be interpreted by the shift of the magnetic axis, since the axis shift due to the finite beta is not included in the ray tracing code. The other possible interpretation might be the presence of the high energy electrons. The calculation of the deposition profile only includes the weakly relativistic effects but not the non thermal component of the plasma.

3. Time Dependent 1-D Electron Transport Code

The limit of applying boxcar analysis is that the data points to analyze should be restricted within the time window where the adiabatic condition is satisfied. It is also reported that total modulated power apt to be lower than the experimentally modulated one [4]. In order to clarify this point and more over to deduce electron thermal diffusivity and its dynamic response to the local plasma parameters, a time dependent one dimensional electron transport code is developed.

This code solves time dependent diffusion equation with the dependence of the electron thermal diffusion coefficient on radius, ρ, local temperature, $T_e(\rho,t)$ and the local temperature gradient, $\frac{\partial T_e(\rho,t)}{\partial \rho}$ included. Figure 5 shows examples of the output from this code. The thermal diffusivity ranges below 1 m^2/s in both cases near the axis. It is noted that including somewhat negative dependence of the diffusivity on the temperature gradient is necessary to reproduce both on axis and off axis cases.

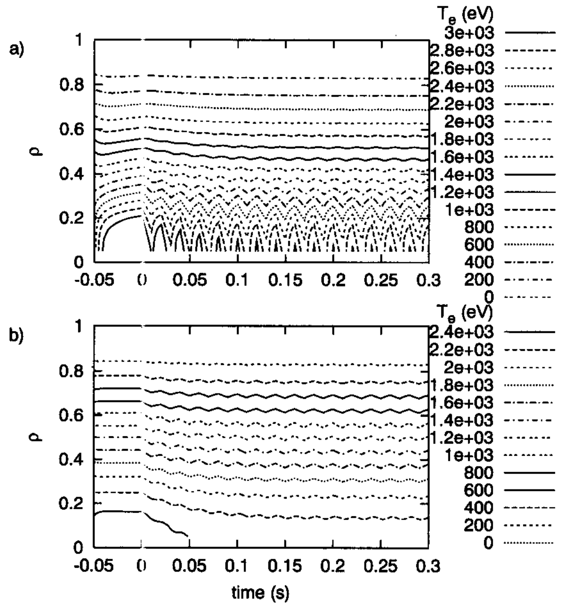

Fig. 5 The result from 1-dimensional time dependent code. The power deposition profile deduced from the boxcar analysis is included for both a) R_{foc} = 3.55 and b) 3.40 m cases. The parameters of diffusion coefficient are selected so that these contour plots well reproduce the Fig. 3.

4. Conclusion

The power deposition profile is the essential key in analyzing and understanding the transport mechanisms. The power deposition profiles are deduced by the boxcar method during the power modulation experiment. These profiles are compared with those calculated from the ray tracing, showing good coincidence. The developed one dimensional time dependent transport code is tried to use for the purpose of deducing the diffusion coefficient and its dependence on the local temperature and local temperature gradient. The deduced thermal diffusivity ranges below 1 m^2/s near the axis, and needs negative dependence on the temperature gradient for the analyzed cases.

References

[1] M. Iwase *et al.*, Jpn. J. Appl. Phys. **37**, 678 (1998).

[2] S. Kubo *et al.*, 'Radio Frequency Power in Plasmas' (Proc. 13th Topical Conf., Melville, New York, 1999 AIP **485**) p. 237.

[3] M. Bornatici *et al.*, Nucl. Fusion **23**, 1153 (1983).

[4] U. Stroth *et al.*, Plasma Phys. Control. Fusion **38**, 661 (1996).